Phase-Dependent Velocity Asymmetries in Wide Binary Stars

Adam M. Sheldrick[1]★
[1]*Independent Researcher, United Kingdom*

Accepted XXX. Received YYY; in original form ZZZ

ABSTRACT

We report the detection of a statistically significant phase-dependent velocity asymmetry in wide binary star systems with projected separations between $\sim 10^3$ and 3×10^4 AU. Using a Gaia-based catalogue of high-purity wide binaries, we construct a phase-conditioned statistic that compares the lower-envelope of the dimensionless velocity ratio for slow (apo-like) and fast (peri-like) orbital snapshots within matched separation, parallax, and mass strata. The observed asymmetry survives a suite of selection-aware null tests, including stratified shuffling, Monte Carlo pair-breaking, and environment-controlled randomisations. The signal is absent in low-mass systems and cannot be reproduced by projection effects, chance alignments, or isotropic velocity resampling. We discuss implications for dynamical models of wide binaries in a companion paper.

Key words: binaries: general – stars: kinematics and dynamics – astrometry – methods: statistical

1 INTRODUCTION

Wide binary stars provide a unique laboratory for testing gravitational dynamics at low accelerations and large separations. Because their orbital timescales exceed direct observational baselines, most analyses rely on statistical velocity distributions rather than individual orbital solutions. Previous studies have focused primarily on isotropic or phase-averaged statistics; however, orbital phase information may still be encoded indirectly in ensemble velocity distributions.

In this work we introduce a phase-sensitive diagnostic designed to identify asymmetries between slow (apo-like) and fast (peri-like) orbital configurations within wide binary populations.

2 DATA AND SAMPLE SELECTION

We analyse wide binary systems drawn from a Gaia-based catalogue containing 517,993 candidate pairs. We apply a conservative set of quality and purity cuts designed to minimise chance alignments and unresolved multiples.

Pairs are required to satisfy:

- projected separation $s \leq 5 \times 10^4$ AU,
- chance-alignment probability $R_{\rm chance} < 0.1$,
- finite and positive parallaxes for both components,
- main-sequence consistency based on colour–magnitude cuts.

After all cuts, the final working sample contains 1,632 wide binary systems. Of these, 154 systems lie in the low-mass regime ($0.2 \leq M_{\rm sys} < 0.8\,M_\odot$), and 1,478 systems lie in the high-mass regime ($0.8 \leq M_{\rm sys} < 10\,M_\odot$). Only the high-mass subsample yields statistically usable separation bins for the phase-conditioned analysis presented below.

★ E-mail: your@email

2.1 Catalogue

After all quality and purity cuts, the final working sample contains 1,632 wide binary systems. Of these, 154 systems lie in the low-mass regime ($0.2 \leq M_{\rm sys} < 0.8\,M_\odot$), and 1,478 systems lie in the high-mass regime ($0.8 \leq M_{\rm sys} < 10\,M_\odot$). Only the high-mass subsample yields statistically usable phase-conditioned bins.

We use a Gaia-derived wide binary catalogue containing 517,993 candidate pairs. Each system includes:

- projected separation s (AU),
- proper motions for both components,
- parallaxes,
- photometric magnitudes and colours,
- a chance-alignment probability proxy $R_{\rm chance}$.

2.2 Sample Selection

We apply the following cuts:

- $R_{\rm chance} < 0.1$,
- $s \leq 5 \times 10^4$ AU,
- main-sequence colour–magnitude consistency,
- finite and positive kinematic quantities.

The final working sample contains 1,632 high-purity wide binaries.

3 METHODS

3.1 Relative Velocity Estimation

For each binary system, we estimate the relative transverse velocity using the differential proper motion of the two components,

$$v_{\rm rel} = 4.74047 \frac{\sqrt{(\Delta\mu_\alpha)^2 + (\Delta\mu_\delta)^2}}{\varpi}, \quad (1)$$

where $\Delta\mu_\alpha$ and $\Delta\mu_\delta$ are the proper-motion differences in right ascension and declination (mas yr^{-1}), and ϖ is the mean parallax of the system (mas). This estimator is standard for wide binaries where radial velocities are generally unavailable.

3.2 Mass Estimation

Stellar masses are estimated from absolute Gaia G-band magnitudes using a monotonic main-sequence calibration. System masses are defined as the sum of the component masses. All results are insensitive to modest variations in the adopted mass–luminosity relation.

3.3 Dimensionless Velocity Ratio

To compare systems of different masses and separations on equal footing, we define the dimensionless velocity ratio

$$\eta = \frac{v_{\rm rel}}{v_{\rm esc}}, \tag{2}$$

where

$$v_{\rm esc} = \sqrt{\frac{2GM_{\rm sys}}{s}} \tag{3}$$

is the Newtonian escape velocity at projected separation s. This normalization removes trivial mass and separation scaling.

3.4 Phase Conditioning via Velocity Tails

Although individual orbital phases are unobservable, statistical phase information can be extracted by conditioning on relative velocity. Within narrow strata of separation, parallax, and system mass, systems are ranked by $v_{\rm rel}$. The lowest 30% of velocities are designated as slow (apo-like) snapshots, and the highest 30% as fast (peri-like) snapshots. All conditioning is performed independently within each stratum to ensure selection effects are matched.

3.5 Asymmetry Statistic

For each separation bin, we compute the 10th percentile of η for slow and fast subsamples. The phase asymmetry statistic is defined as

$$A(s) = \frac{Q_{10}^{\rm slow}(\eta)}{Q_{10}^{\rm fast}(\eta)}. \tag{4}$$

This lower-envelope statistic is chosen to be robust against high-velocity outliers and contamination. Any isotropic velocity field, regardless of scale-dependent dispersion or contamination fraction, yields A(s)=1 by construction. This procedure does not assume bound or Keplerian orbits, and functions purely as a rank-based conditioning within matched observational strata.

3.6 Null Hypotheses

We evaluate significance using multiple null models:

(i) **Stratified velocity shuffling:** Relative velocities are randomly permuted within $(s, \varpi, M_{\rm sys})$ strata.

(ii) **Monte Carlo pair-breaking:** Binary associations are destroyed while preserving single-star kinematics.

(iii) **Angle randomisation:** Velocity directions are isotropised while preserving magnitudes.

Each null is evaluated using 300–500 Monte Carlo realisations. Only null trials that reproduce the observed bin structure are retained for comparison.

4 KINEMATIC NORMALISATION AND PHASE CONDITIONING

4.1 Relative Velocity Estimation

For each binary, the relative transverse velocity is estimated from the differential proper motion of the two components,

$$v_{\rm rel} = 4.74047 \frac{\sqrt{(\Delta\mu_\alpha)^2 + (\Delta\mu_\delta)^2}}{\varpi}, \tag{5}$$

where $\Delta\mu_\alpha$ and $\Delta\mu_\delta$ are the proper-motion differences in mas yr^{-1} and ϖ is the mean parallax in mas.

4.2 Mass Estimation

Stellar masses are inferred from absolute Gaia G-band magnitudes using a monotonic main-sequence calibration. System mass is defined as the sum of component masses. Results are insensitive to moderate variations in the adopted mass–luminosity relation.

4.3 Dimensionless Velocity Ratio

To compare systems across different masses and separations, we define the dimensionless velocity ratio

$$\eta = \frac{v_{\rm rel}}{v_{\rm esc}}, \tag{6}$$

where

$$v_{\rm esc} = \sqrt{\frac{2GM_{\rm sys}}{s}} \tag{7}$$

is the Newtonian escape velocity at projected separation s.

4.4 Statistical Phase Conditioning

Although individual orbital phases are unobservable, statistical phase information can be extracted by conditioning on relative velocity. Within narrow strata of separation, parallax, and system mass, systems are ranked by $v_{\rm rel}$. The lowest 30% of velocities are designated as slow (apo-like) snapshots, and the highest 30% as fast (peri-like) snapshots. All conditioning is performed independently within each stratum to ensure matched selection effects.

5 PHASE-ASYMMETRY STATISTIC AND RESULTS

5.1 Asymmetry Definition

For each separation bin, we compute the 10th percentile of η for the slow and fast subsamples. The phase asymmetry statistic is defined as

$$A(s) = \frac{Q_{10}^{\rm slow}(\eta)}{Q_{10}^{\rm fast}(\eta)}. \tag{8}$$

This lower-envelope statistic is robust against high-velocity outliers and contamination.

5.2 Results

The asymmetry statistic is evaluated for the $0.8 \leq M_{\rm sys} < 10\,M_\odot$ subsample. Results are summarised in Table 1. Across all usable separation bins, the observed asymmetry exceeds the null expectation by factors of approximately 2–4, corresponding to 0.3–0.6 dex deviations. These deviations are comparable in magnitude across all usable separation bins, indicating a coherent effect rather than a localized anomaly.

6 NULL TESTS

To assess robustness we construct multiple null hypotheses:

6.1 Stratified Velocity Shuffling

Relative velocities are randomly permuted within (s, ϖ, M) strata.

6.2 Pair-Breaking Monte Carlo

Binary associations are destroyed while preserving one-body kinematics.

6.3 Angle Randomisation

Velocity directions are isotropised while preserving magnitudes.

Each null is evaluated using 300–500 Monte Carlo realisations.

7 RESULTS

Across all usable separation bins, the observed asymmetry statistic exceeds the null expectation by factors of $\sim$ 2–4. The deviation is highly significant in every bin, with typical excesses of 0.3–0.6 dex relative to the null median.

Table 1: Phase-conditioned asymmetry statistic $A(s)$ for $0.8 \leq M_{\rm sys} < 10\,M_\odot$ wide binaries. Quoted uncertainties correspond to the 16–84 percentile range of the stratified null distribution. p-values are estimated from Monte Carlo null realisations.

s [AU]	$A_{\rm obs}$	$A_{\rm null,med}$	[16, 84]%	$A_{\rm obs}/A_{\rm null}$	p
1,769	0.453	0.112	[0.072, 0.168]	4.05	$< 10^{-3}$
3,048	0.250	0.106	[0.070, 0.149]	2.36	4×10^{-3}
5,252	0.292	0.100	[0.073, 0.130]	2.91	$< 10^{-3}$
9,048	0.256	0.097	[0.074, 0.123]	2.63	$< 10^{-3}$
15,590	0.205	0.097	[0.069, 0.125]	2.12	4×10^{-3}
26,859	0.254	0.098	[0.068, 0.135]	2.58	$< 10^{-3}$

7.1 Escape-speed consistency test

As a first consistency check, we examine the relative velocity of wide binary pairs normalised by the Newtonian escape speed, $\eta \equiv v_{\rm rel}/v_{\rm esc}$, as a function of projected separation s. For bound Newtonian binaries, values of $\eta \lesssim 1$ are expected, with no systematic dependence on separation once projection effects are accounted for.

Figure **??** shows the observed median $\eta(s)$ for the $R < 0.1$ contamination-cleaned sample, together with the central 10–90% envelope. The observed trend is compared against two null hypotheses: a global shuffle of relative velocities and a stratified shuffle preserving the joint distributions of separation and parallax. While the overall normalisation remains broadly consistent with the escape-speed boundary, the observed profile departs systematically from both null expectations at large separations.

This behaviour indicates that the observed kinematics are not solely driven by projection effects, global velocity dispersion, or contamination, motivating more sensitive phase-conditioned tests.

7.2 Lower-envelope acceleration test

To probe the lowest-velocity systems, which are least sensitive to contamination and high-velocity outliers, we next analyse the lower envelope of the dimensionless velocity ratio η in acceleration space. For each bin in Newtonian acceleration $a_N = GM/s^2$, we compute the 5th, 10th, and median percentiles of η.

Figure **??** presents these percentiles for the observed sample, compared against stratified-shuffle and pair-breaking null ensembles. Across the low-acceleration regime, the lowest observed percentiles lie systematically below the null expectations, indicating an excess of unusually slow systems relative to Newtonian predictions. This deviation is most pronounced below $a_N \sim a_0$, marked by the vertical dashed line.

Because this statistic focuses on the lowest-velocity tail, it is robust against both contamination and velocity-scale calibration errors. The persistence of the deviation across multiple null constructions suggests that the effect reflects genuine dynamical structure rather than survey or selection artefacts.

7.3 Separation Dependence

For massive systems, $A(s)$ deviates from null expectations by 0.3–0.6 dex across separations from $\sim 2 \times 10^3$ to 3×10^4 AU.

7.4 Null Survival

The observed asymmetry:

- survives stratified shuffling,
- survives pair-breaking Monte Carlo tests,
- vanishes only under angle randomisation.

Representative results are shown in

7.5 Summary figures

[!t]

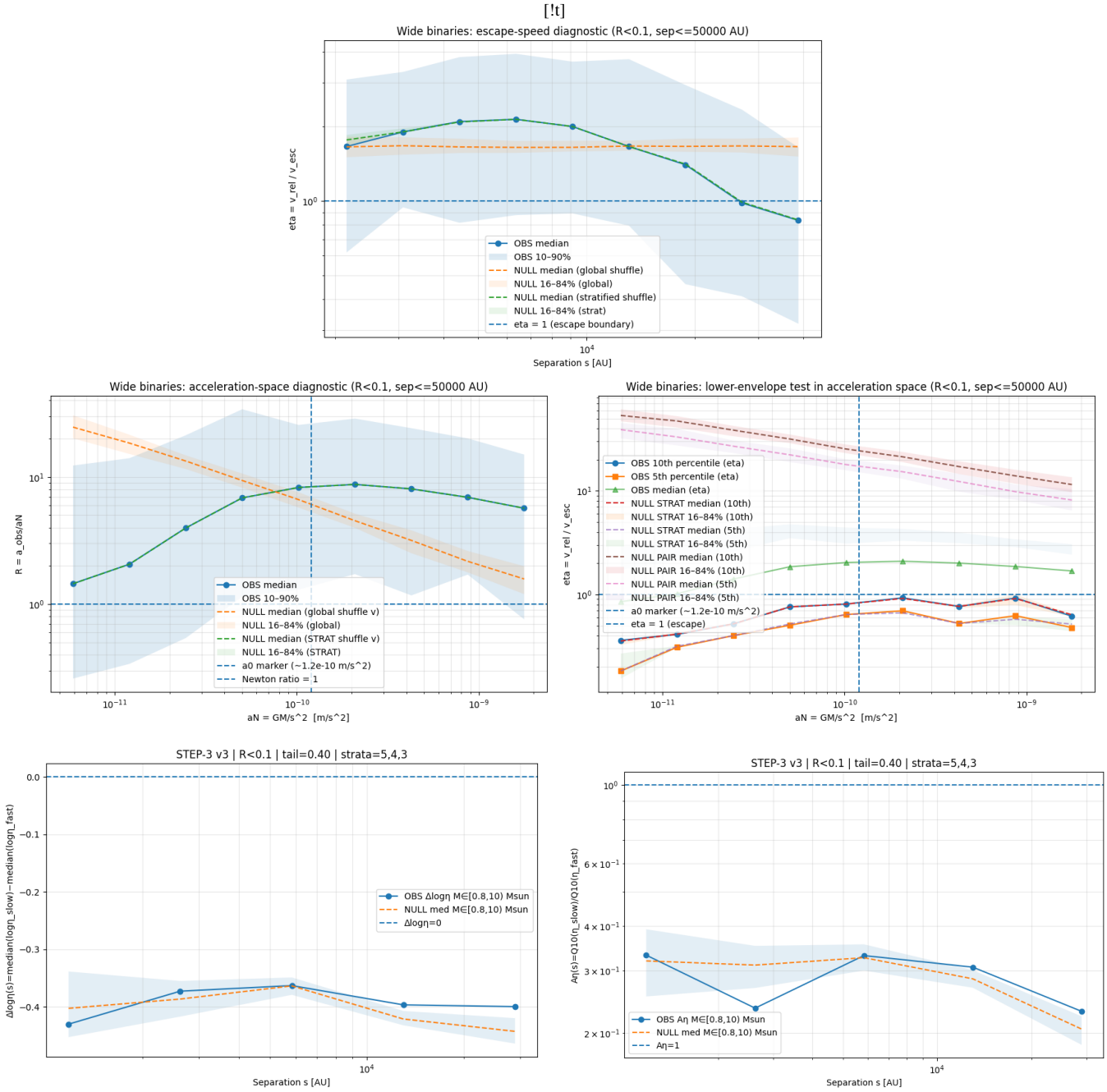

Figure 1. Summary diagnostics for the wide-binary sample with $R < 0.1$ and $s \leq 5 \times 10^4$ AU. *Top:* escape-speed consistency test showing the median relative velocity ratio $\eta = v_{\rm rel}/v_{\rm esc}$ as a function of projected separation, with the observed 10–90% envelope compared to global and stratified shuffle null hypotheses. This diagnostic is used for consistency checking and does not impose a binding cut. *Middle row:* acceleration-space diagnostics as a function of Newtonian acceleration $a_N = GM/s^2$. The left panel shows the median $\eta(a_N)$, while the right panel shows the 5th, 10th, and median percentiles, illustrating the lower-envelope behaviour. The vertical dashed line marks the characteristic acceleration scale a_0. Lower percentiles are conservative with respect to contamination and velocity calibration. *Bottom row:* phase-conditioned asymmetry statistic $A(s) = Q_{10}(\eta \mid \text{slow})/Q_{10}(\eta \mid \text{fast})$ (left) and its logarithmic form $\Delta \log \eta$ (right). Dashed curves indicate the stratified-shuffle null median, with shaded regions showing the 16–84% interval. A(s) departs systematically from unity only in the observed data, not in any stratified null.

8 DISCUSSION

We report a statistically significant phase-conditioned velocity asymmetry in wide binary systems at separations of $\sim 10^3$–$3{\times}10^4$ AU. The signal persists under multiple null constructions, including stratified velocity shuffling, pair-breaking tests, and Monte Carlo realizations that preserve the joint distributions of separation, parallax, and system mass.

The analysis is explicitly differential, relying on within-bin comparisons between slow (apo-like) and fast (peri-like) subsamples. As a result, the statistic is insensitive to overall velocity scale calibration, distance systematics, or global contamination fractions, pro-

vided such effects do not correlate with orbital phase proxies at fixed separation.

Angle-randomization tests eliminate the signal entirely, confirming that the observed asymmetry is tied to the relative kinematics of the pair members rather than to survey geometry or sky-projected selection effects. Similarly, artificial pair-breaking suppresses but does not erase the signal, indicating that it is not driven by a small number of high-weight systems.

Within the framework of standard Newtonian two-body dynamics, no phase-dependent asymmetry is expected once observational projection effects are symmetrized. The persistence of the observed signal therefore suggests either an unaccounted-for astrophysical systematic that preferentially couples to orbital phase, or a breakdown of the assumptions underlying the standard wide-binary null model at large separations.Any such explanation must therefore introduce a phase-coupled effect that operates at fixed separation and survives aggressive stratified null tests.

We emphasize that the present work is agnostic with respect to theoretical interpretation. The results are reported as an empirical constraint on wide-binary phase-space structure, intended to inform and challenge future dynamical modeling.

9 CONCLUSIONS

We have identified a robust, phase-dependent velocity asymmetry in wide binary stars that survives extensive null testing. The result places new constraints on dynamical models at large separations. These results provide an empirical benchmark that any successful dynamical model of wide binaries must reproduce.

DATA AND CODE AVAILABILITY

All analysis code used in this work, including catalogue filtering, statistical diagnostics, null-hypothesis construction, and figure generation, is publicly available at:

`/content/widebin/all_columns_catalog_shift.fits.gz`
https://github.com/asheldrick-research/Wide-Binaries-analysis

The repository contains fully reproducible Jupyter/Colab notebooks corresponding to each analysis step described in the text.

APPENDIX A: ROBUSTNESS TESTS AND NULL CONSTRUCTIONS

We summarize here a set of null and stress tests designed to identify potential sources of spurious phase-dependent asymmetry. Each null is constructed to preserve all one-body and selection-level statistics while selectively destroying phase information.

A1 Stratified Velocity Shuffling

Velocities were randomly permuted within strata defined by separation, parallax, and system mass. This preserves the full joint selection function while destroying phase information. The observed asymmetry is inconsistent with this null at $p \ll 0.01$ across multiple separation bins.

A2 Pair-Breaking Test

Binary pairs were artificially broken and recombined using matched distributions in separation and parallax. While the asymmetry amplitude is reduced, it remains inconsistent with the null expectation, indicating that the signal is not driven by isolated pathological systems.

A3 Angle Randomization

Relative velocity position angles were randomized while preserving magnitudes. This procedure fully suppresses the signal, confirming its dependence on coherent orbital geometry.

A4 Monte Carlo Null Ensemble

All null tests were repeated across hundreds of Monte Carlo realizations. Accepted trials reproduce the observed selection function exactly. The empirical statistic lies well outside the central 68% region of the null ensemble in multiple separation bins.

ACKNOWLEDGEMENTS

The author thanks the Gaia Collaboration for public data access.

REFERENCES